

# Growth and spectral properties of Yb,Tm:YAG crystal

Xiaodong Xu<sup>\*</sup>, Feng Wu, Wenwei Xu, Yanhua Zong, Xiaodan Wang,  
Zhiwei Zhao, Guoqing Zhou, Jun Xu

Shanghai Institute of Optics and Fine Mechanics, Chinese Academy of Sciences, P.O. Box 800-211, Shanghai 201800, People's Republic of China

Received 10 July 2007; received in revised form 15 August 2007; accepted 16 August 2007

Available online 28 August 2007

## Abstract

The YAG crystal codoped with Yb<sup>3+</sup> and Tm<sup>3+</sup> has been grown by Czochralski (Cz) method. The crystal structure of the crystal has been determined by X-ray diffraction analysis. The absorption and emission spectra of Yb,Tm:YAG crystal at room temperature have also been studied. The emission cross-sections have been calculated by Fuechtbauer-Ladenburg formula and reciprocity method.

© 2007 Elsevier B.V. All rights reserved.

PACS: 42.70.Hj; 81.10.Fq; 87.64.Ni

Keywords: Oxide materials; Crystal growth; Optical properties

## 1. Introduction

Recent years have witnessed the development of solid-state lasers operating in the 1.6–2.0 μm spectral region. 1.6–2.0 μm lasers have gain wide interests and applications in such fields as multiple lidar, telecommunication and atmospheric sensing because of strong absorption by water and water vapor in this wavelength region. 1.6–2.0 μm lasers are safe to human eyes and thus are also widely used in medicine. Most solid-state 1.6–2.0 μm laser operations are based on transition  $^3F_4 \rightarrow ^3H_6$  in thulium ions and the performance of the thulium ions in a number of solid-state host has been widely studied and laser operation has been successfully realized [1–13].

However, diode-pumped thulium doped lasers are typical of high laser threshold and low laser efficiency due to the weak absorption of Tm<sup>3+</sup> ions at the pumping wavelength region. Yb<sup>3+</sup> ions are excellent sensitizers to improve the laser performance of Tm<sup>3+</sup> doped crystals by absorbing the pump light and then transferring energy to Tm<sup>3+</sup> ions [14]. Yb<sup>3+</sup> as a 4f<sup>13</sup> ion has a very simple energy structure with only two manifolds, the ground state  $^2F_{7/2}$  and excited state  $^2F_{5/2}$ , which are separated by about 10,000 cm<sup>-1</sup> [15]. Moreover, Yb<sup>3+</sup> doped in YAG possess large ground state stark splitting and thus has a quasi-three

energy structure, which enable broad and intense absorption band corresponding the transition of  $^2F_{7/2} \rightarrow ^2F_{5/2}$  in Yb<sup>3+</sup> ions and effectively increase the population of the upper level of Tm<sup>3+</sup> ions by nonradiative energy transfer from ytterbium to thulium. YAG crystals are also easy to grow by Czochralski method and widely used. All of these advantages over other matrices make Yb,Tm-codoped YAG a promising laser material with low threshold and high efficiency compared with Tm<sup>3+</sup> doped YAG.

In this work, we presented the growth and crystal structure properties of Yb,Tm:YAG. Room temperature absorption and emission properties of this crystal were studied.

## 2. Experiment

According to the Y<sub>2</sub>O<sub>3</sub>–Al<sub>2</sub>O<sub>3</sub> phase diagram, YAG crystal melts congruently at 1980 °C, and Yb,Tm:YAG crystal in this work was grown by Czochralski method from an inductively heated iridium crucible. The Yb<sup>3+</sup> and Tm<sup>3+</sup> concentrations are 5 and 4 at.%, respectively. Good quality of raw materials is quite important to high-quality of crystals. The starting material was obtained by mixing powders of Yb<sub>2</sub>O<sub>3</sub>, Tm<sub>2</sub>O<sub>3</sub>, Y<sub>2</sub>O<sub>3</sub> and Al<sub>2</sub>O<sub>3</sub>, all of which is at least 99.999% in purity. Then the well mixed powder was pressed into blocks which will be sent into a corundum to be sintered at 1400 °C for 24 h, the purpose of this procedure is to facilitate the formation of YAG polycrystal.

<sup>\*</sup> Corresponding author. Tel.: +86 21 69918485; fax: +86 21 69918607.  
E-mail address: xdxu79@yahoo.com.cn (X. Xu).

The rods were placed in a iridium crucible of 70 mm in diameter and 50 mm in height, we chose a  $\langle 111 \rangle$  oriented pure YAG as a seed, the axial temperature gradient was 30–40 °C/cm. 5N nitrogen gas was flowed continuously into the iridium crucible as neutral atmosphere to prevent oxidization, the solid-melt growth boundary was convex to the melt so that the impurities were reduced or eliminated. The pulling rate and rotation rate was 1–2 mm/h and 10–20 rpm, respectively.

The crystal structure of the as-grown crystal was examined with a D/MAX 2550V powder X-ray diffractometer (XRD). The diffractometer using RINT2000 vertical goniometer (40 kV, 40 mA with fixed monochromator and continuous scanning) in this process, the divergence slit is 1° and the receive slit 0.3 mm step size is 0.02° and the scanning range is 10–90° ( $2\theta$ ).

Sample used in spectral analysis was cut from the boules with two surfaces perpendicular to the  $\langle 111 \rangle$  axis and polished to spectral quality. The thickness of the sample was 0.68 mm. The room temperature absorption spectrum was obtained by Jasco V-570 UV/vis/NIR spectrophotometer in the wavelength range from 250 to 2000 nm; the resolution is 1 nm. The room temperature emission spectrum was obtained under 970 nm excitation with InGaAs laser diode by a Nikon G250 monochromator and PbS detector. The decay time was measured by a Yocogawa DL1620 digital oscilloscope.

### 3. Results and discussion

Fig. 1 shows the as-grown Yb,Tm:YAG crystal boule. The crystal is about 30–35 mm in diameter and 30 mm in length. When the 20 mW He–Ne laser beam passed through the as-grown Yb,Tm:YAG, the light beam was almost unseen by eyes, which indicated very few scattering particles in Yb,Tm:YAG crystal.

X-ray powder diffraction results of Yb,Tm:YAG and pure YAG single crystal at room temperature are shown in Fig. 2. From Fig. 2, we can see that the locations of Yb,Tm:YAG peaks are almost the same as that of pure YAG although the strength of peaks is different. The Yb,Tm:YAG crystal has the same structure as the pure YAG. The calculated lattice constant for

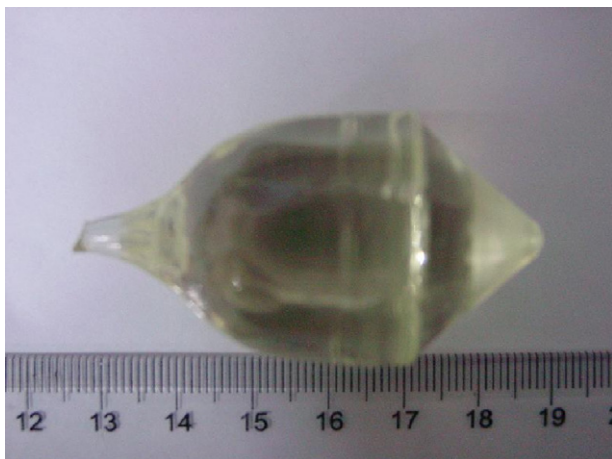


Fig. 1. The photograph of as-grown Yb,Tm:YAG crystal boule.

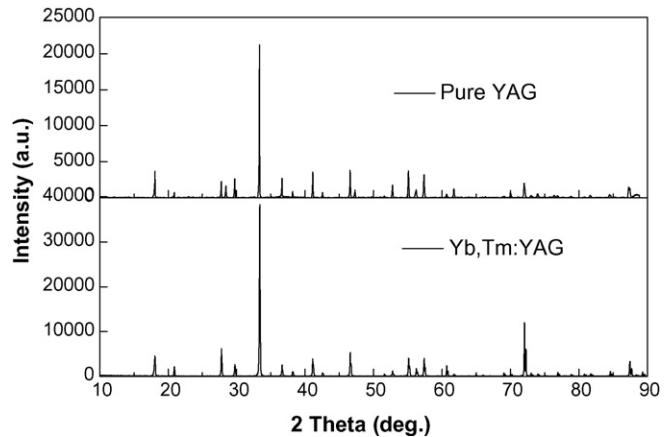


Fig. 2. The X-ray power diffraction pattern of pure YAG and Yb,Tm:YAG.

Yb,Tm:YAG crystal is about 1.2125 nm, which is very close to that of pure YAG (lattice constant for pure YAG is 1.2012 nm).

The absorption spectrum of Yb,Tm:YAG crystal from 250 to 2000 nm at room temperature is shown in Fig. 3. From Fig. 3, we can see that seven bands are associated with  $\text{Tm}^{3+}$  transitions from the  $^3\text{H}_6$  ground state to  $^3\text{P}_2$ ,  $^1\text{D}_2$ ,  $^3\text{F}_4$ ,  $^3\text{H}_5$ ,  $^3\text{H}_4$ ,  $^3\text{F}_3$ – $^3\text{F}_2$ ,  $^1\text{G}_4$  excited states, respectively, and the band around 0.9–1.0  $\mu\text{m}$  is associated with the  $^2\text{F}_{7/2} \rightarrow ^2\text{F}_{5/2}$  transition of  $\text{Yb}^{3+}$ . The absorption cross-section is  $0.82 \times 10^{-20} \text{ cm}^2$  at 940 nm and  $0.85 \times 10^{-20} \text{ cm}^2$  at 1624 nm. Though only one band is attributed to the transition of  $^2\text{F}_{7/2}$  to  $^2\text{F}_{5/2}$  in  $\text{Yb}^{3+}$  ions, the band is intense and much wider than any other bands associated with transition from the ground state to upper levels in  $\text{Tm}^{3+}$  ions, the strong absorption derives from the large ground state stark splitting of  $\text{Yb}^{3+}$ , making  $\text{Yb}^{3+}$  an excellent sensitizer to absorb the pump light.

The emission spectrum ranging from 1600 to 2200 nm was obtained under 970 nm pumping (presented at Fig. 4), and the emission bands correspond to the transition  $^3\text{F}_4 \rightarrow ^3\text{H}_6$  of  $\text{Tm}^{3+}$ . Fluorescence decay curve for the  $^3\text{F}_4 \rightarrow ^3\text{H}_6$  energy transition was shown in Fig. 5. The fluorescence lifetime is measured to be 13.2 ms, which is much more larger than that of the  $\text{Tm}^{3+}$  in Tm:YAG crystal.

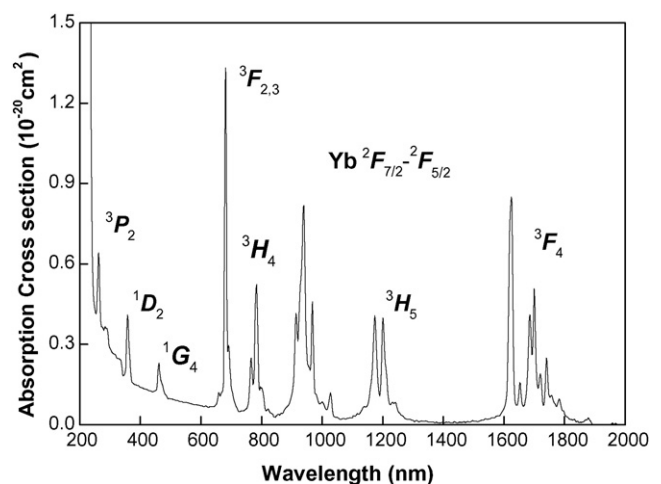


Fig. 3. Room temperature absorption spectrum of Yb,Tm:YAG single crystal.

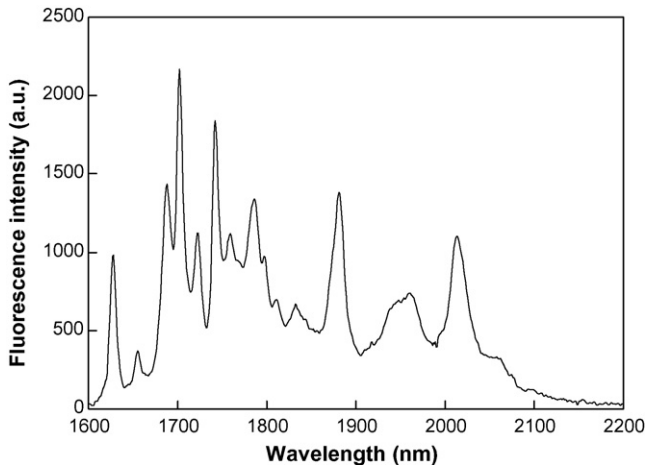


Fig. 4. Room temperature emission spectrum of Yb,Tm:YAG single crystal.

The stimulated emission cross-section of  ${}^3F_4 \rightarrow {}^3H_6$  transition can be calculated by the Fuechtbauer-Ladenburg formula [16]:

$$\sigma_{em}(\lambda) = \frac{\lambda^5 I(\lambda)}{8\pi n^2 c \tau \int I(\lambda) \lambda d\lambda}$$

where  $I(\lambda)$  is the emission spectral intensity at different wavelength of  $Tm^{3+}$  ions,  $c$  the light velocity,  $n$  the refractive index, and  $\tau$  is the radiative lifetime of the upper laser level. The calculated emission cross-section is presented in Fig. 6. The maximum value of emission cross-section is  $0.19 \times 10^{-20} \text{ cm}^2$  at 2014 nm.

The emission cross-section can also be calculated from the ground state absorption cross-section using the reciprocity method [16]:

$$\sigma_{em}(\lambda) = \sigma_{abs}(\lambda) \frac{Z_l}{Z_u} \exp\left[\frac{E_{ZL} - (hc/\lambda)}{kT}\right]$$

In the above equation,  $\sigma_{abs}(\lambda)$  is the absorption cross-section,  $Z_l$  and  $Z_u$  are partition functions of lower and upper manifolds, respectively.  $E_{ZL}$  is the zero-line energy, and is defined as the energy difference between the lowest Stark level of the

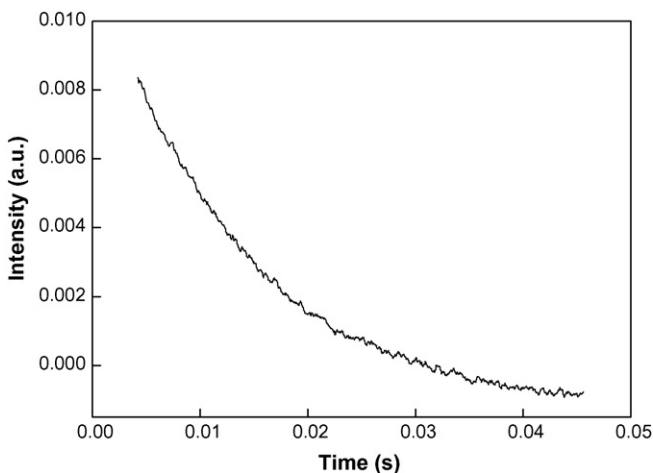


Fig. 5. Decay curves of the  ${}^3F_4$  manifold of the  $Tm^{3+}$  in Yb,Tm:YAG crystal.

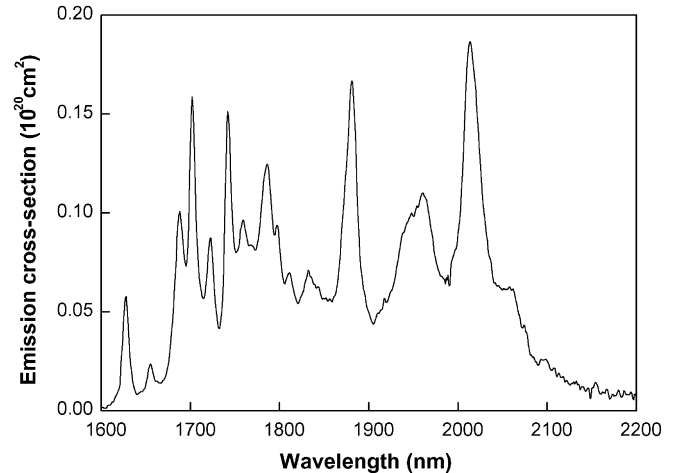


Fig. 6. The emission cross-section derived by the Fuechtbauer-Ladenburg method.

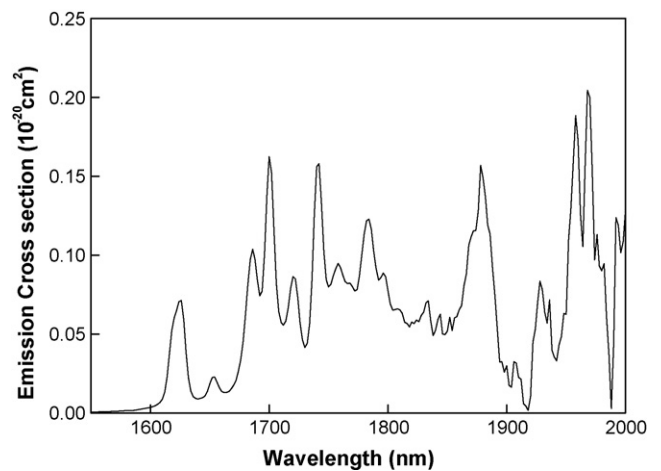


Fig. 7. The emission cross-section derived by the reciprocity method.

upper manifold and the lowest Stark level of the lower manifold. The stark levels of manifolds are provided by previous literature [17]. The calculated emission cross-section is shown in Fig. 7. The emission cross-section is  $0.16 \times 10^{-20} \text{ cm}^2$  at 1878 nm. From Figs. 6 and 7, we can see that the emission cross-sections are comparable before 1900 nm. The emission cross-sections derived by the reciprocity method is influenced by the baseline at the wavelength larger than 1900 nm, so we consider that the emission cross-sections are inaccurate when the wavelength is larger than 1900 nm.

#### 4. Conclusion

Yb,Tm:YAG crystal with good optical quality was grown by Czochralski method, the crystal has the same structure as YAG crystal. The absorption spectrum from 250 to 2000 nm and emission spectrum around 1600 nm of Yb,Tm:YAG were studied at room temperature. The experimental fluorescence lifetime was 13.2 ms. The emission cross-section from 1600 to 2200 nm has been calculated by Fuechtbauer-Ladenburg formula and the peak emission cross-section was  $0.19 \times 10^{-20} \text{ cm}^2$

at 2014 nm. The emission cross-section has been also calculated by reciprocity method and the peak emission cross-section was  $0.16 \times 10^{-20} \text{ cm}^2$  at 1878 nm.

## References

- [1] K. Scholle, E. Heumann, G. Huber, *Laser Phys. Lett.* 1 (2004) 285–290.
- [2] G. Galzerano, F. Cornacchia, S. Parisi, et al., *Opt. Lett.* 30 (2005) 854–856.
- [3] V. Petrov, F. Güell, J. Massons, J. Gavalda, et al., *IEEE J. Quantum Electron.* 40 (2004) 1244–1251.
- [4] C.P. Wyss, W. Lüthy, H.P. Weber, et al., *IEEE J. Quantum Electron.* 34 (1998) 2380–2382.
- [5] S.N. Bagaev, S.M. Vatik, A.P. Maiorov, et al., *Quantum Electron.* 20 (2000) 310–314.
- [6] A. Braud, P.Y. Tigreat, J.L. Doualan, et al., *Appl. Phys. B* 72 (2001) 909–912.
- [7] N.I. Borodin, P.V. Kryukov, A.V. Popov, et al., *Quantum Electron.* 35 (2005) 511–514.
- [8] P. Camy, J.L. Doualan, S. Renard, et al., *Opt. Commun.* 236 (2004) 395–402.
- [9] C. Li, J. Song, D. Shen, et al., *Opt. Express* 4 (1999) 12–18.
- [10] X. Mateos, J. Liu, H. Zhang, et al., *Phys. Status Solidi (a)* 4 (2006) R19–R21.
- [11] J. Foing, E. Scheer, B. Viana, et al., *Appl. Opt.* 37 (1998) 4857–4861.
- [12] R. Moncorgé, N. Garnier, Ph. Kerbrat, et al., *Opt. Commun.* 141 (1997) 29–34.
- [13] E.C. Honea, R.J. Beach, S.B. Sutton, et al., *IEEE J. Quantum Electron.* 33 (1997) 1592–1600.
- [14] L.E. Batay, A.A. Demidovich, A.N. Kuzmin, et al., *Appl. Phys. B* 75 (2002) 457–461.
- [15] W.F. Krupke, *IEEE J. Sel. Top. Quantum Electron.* 6 (2000) 1287–1296.
- [16] S.A. Pain, L.L. Chase, L.K. Smith, et al., *IEEE J. Quantum Electron.* 28 (1992) 2619–2630.
- [17] J.B. Gruber, et al., *Phys. Rev. B* 40 (1989) 9464–9478.